DETERMINING LONGWAVE RADIATIVE PROPERTIES OF FLAT SHADING MATERIALS

N. A. Kotey, J.L. Wright and M. R. Collins
Department of Mechanical and Mechatronics Engineering, University of Waterloo
200 University Avenue West, Waterloo, ON N2L 3G1
Phone: 519-888-4567 ext 33885
Corresponding Email Address:nakotey@engmail.uwaterloo.ca

Topic Area: Integration of Solar Energy Systems into Buildings (Oral Presentation)

ABSTRACT

Solar gain through fenestration has a significant impact on building peak load and annual energy consumption. Shading devices, attached to fenestration, offer a cost effective strategy in controlling solar gain. The performance of a particular shading device is dependent on solar optical and longwave radiative properties of the device. The current study considers longwave properties of three flat shading materials; drapery fabrics, insect screens and roller blinds. Each of these materials consists of a structure (i.e., yarn, wire, sheet) that is opaque with respect to longwave (infrared) radiation and each material is likely to have some openness. Material emittance and longwave transmittance measurements were taken with an infrared reflectometer using two backing surfaces. The results show emittance and longwave transmittance to be simple functions of openness, emittance and longwave transmittance of the structure. This is especially useful because openness can be determined from solar transmittance measurements while emittance and longwave transmittance of the structure was found to be constant for each category of shading material.

INTRODUCTION

Shading devices offer a cost effective strategy in reducing solar heat gain through windows. As such, the ability to accurately quantify the reduction in cooling load that these devices deliver would be an asset to HVAC engineers in particular and building designers in general.

The energy performance for windows with shading devices can be modeled using a two step procedure. In the first step, solar radiation is considered. This requires the determination of the solar optical properties of each layer in the glazing/shading system. Shading layers are characterized by making the assumption that each layer, whether homogeneous or not, can be represented by an equivalent homogenous layer that is assigned spatially-averaged "effective" optical properties. This approach has been used in a number of studies (e.g., Parmelee and Aubele 1952, Rheault and Bilgen 1989, Pfrommer et al. 1996, Rosenfeld et al. 2000, Yahoda and Wright 2004, 2005) and has been shown to provide accurate characterization of venetian blinds (e.g., Kotey et al. 2008).

A careful consideration of solar radiation incident on a shading layer with some openness reveal that a portion of the incident radiation passes undisturbed through openings in a shading layer and the remaining portion is intercepted by the structure of the layer. The structure may consist of yarn, slats, or some other material. The portion of the intercepted radiation that is not absorbed will be scattered and will leave the layer as an apparent reflection or transmission. These scattered components are assumed to be uniformly diffuse. In addition, a shading layer will generally transmit longwave radiation (i.e., it is diathermanous), by virtue of its openness, and effective longwave properties are assigned accordingly. The effective properties can then be used as part of a multilayer calculation that considers beam and diffuse components of solar radiation as they interact with a multilayer assembly (e.g., Wright and Kotey 2006). This calculation estimates the system solar transmission and absorbed solar components. The absorbed solar components appear as energy source terms in the second step – the heat transfer analysis.

The heat transfer analysis involves the formulation of energy balance equations and requires both longwave properties and convective heat transfer coefficients as input. The simultaneous solution of the energy balance equations yields the temperature as well as the convective and radiative fluxes.

For shading layers such as venetian blinds and pleated drapes, the determination of the effective longwave properties is a two step procedure. First step involves the measurement of the longwave properties of the slat or the fabric. These measured properties are used in a net radiation analysis to estimate the effective longwave properties of the venetian blind or the pleated drape in the second step

(Yahoda and Wright 2005, Kotey et al. 2009d). On the hand, the effective longwave properties of flat shading layers such as roller blinds and insect screens can be measured directly.

In the current study, spectral measurements of normal-hemispherical longwave reflectance and transmittance were obtained for three flat shading materials; drapery fabrics, insect screens and roller blinds using an infrared reflectometer. The spectral data showed that the shading materials are generally not spectrally selective. Since the aim of the current study was to generate total (spectral-averaged) properties for building energy simulation, no spectral data are presented. The total properties, including emittance, were calculated with respect to blackbody spectrum at a given temperature (ASTM E408-71 1971). The procedure entailed the solution of two simultaneous equations resulting from the reflectance measurements with the sample backed by two surfaces with different reflectance values. A similar procedure was used by Christie and Hunter (1984) to determine the longwave properties of thin diathermanous films using DB-100 Infrared Reflectometer. Having obtained emittance and longwave transmittance of each shading material, it was recognised that these quantities are simple functions of openness, emittance and longwave transmittance of the structure. Furthermore, the emittance and the longwave transmittance of the structure were found to be constant for each category of shading material.

TEST SAMPLES

A wide variety of commercially available shading materials were selected for testing. This includes samples of drapery fabrics, roller blinds and insect screens. The dimensions of each sample were 5 cm by 5 cm. Solar beam-beam transmittance, τ_{bb}, was obtained from spectrophotometer measurements (Kotey et al. 2009a, 2009b and 2009c). At normal incidence τ_{bb} is equivalent to the openness, A_o, which is defined as the ratio of the open area to the total area of the shading material. The shading materials tested are briefly described below.

Drapery Fabrics

A variety of drapery fabrics were obtained with the primary aim of locating samples that fit into each of the nine designations described by Keyes (1967). With the exception of designation IIID which could not be located, all designations were obtained. Also included in the sample set was a sheer fabric which did not fall into any of the customary designations. The thicknesses of the fabric samples ranged from 0.1 mm to 1.0 mm. Table 1 summarises the type, colour and openness of each fabric sample considered.

Table 1. Description of Fabric Samples

Type	Colour	Openness
Sheer (None)	Cream	0.44
Open weave, light coloured (IL)	White	0.24
Semi-open weave, light coloured (IIL)	White	0.01
Closed weave, light coloured (IIIL)	White	0.01
Open weave, medium coloured (IM)	Brown	0.34
Semi-open weave, medium coloured (IIM)	Green	0.02
Closed weave, medium coloured (IIIM)	Blue	0.01
Open weave, dark coloured (ID)	Black	0.20
Semi-open weave, dark coloured (IID)	Black	0.05

Roller Blinds

The roller blinds tested were grouped into two categories - open weave and closed weave. Six different samples were selected for testing, representing the majority of roller blinds currently in use. The thicknesses of the samples ranged from 0.3 mm to 0.8 mm. The type, colour and the openness of each sample are summarised in Table 2.

Table 2. Description of Roller Blind Samples

Type	Colour	Openness
Open weave vinyl coated fibreglass	White	0.13
Open weave vinyl coated fibreglass	Black	0.12
Open weave 25% polyester, 75% PVC on polyester	Chalk	0.08
Open weave 25% polyester, 75% PVC on polyester	Ebony	0.06
Closed weave, 12 oz fibreglass, duplex, room darkening, opaque	Black on one side, white on the other side	0.00
Closed weave, 84% polyester, 16% linen, translucent	Natural glacier	0.00

Insect Screens

Table 3 summarises the eight different samples of insect screens tested. With the exception of one screen that was made from fibre glass, all other screens were made from stainless steel and were either shiny or dark coloured. The thickness of each sample is equivalent to the wire diameter. See Table 3. The samples considered represent a wide range of insect screens currently in use as window attachments.

EXPERIMENTAL PROCEDURE

Infrared Reflectometer

A commercially available FTIR (Fourier Transform Infrared Spectroscopy) reflectometer, SOC 400T, was used in this study. It is a portable, self calibrating instrument with a reflectance repeatability of ±1% and a spectral resolution selectable from 4 to 32 reciprocal centimetres. The reflectometer is designed to measure normal-hemispherical reflectance of an opaque surface in the wavelength range of $2.0 < \lambda < 25.0$ μm (infrared region). The instrument collects many infrared spectra over a short period of time.

Table 3. Description of Insect Screen Samples

Type	Colour	Openness
150 mesh 0.0026 in.dia shiny	Shiny	0.36
120 mesh 0.0026 in. dia shiny	Shiny	0.46
20 mesh 0.016 in. dia shiny	Shiny	0.49
60 mesh 0.0045 in. dia shiny	Shiny	0.52
20 mesh 0.010 in. dia bluegray	Blue-grey	0.63
26 mesh 0.006 in. dia charcoal	Charcoal-black	0.70
18 mesh 0.009 in. dia charcoal	Charcoal-black	0.62
18 mesh 0.012 in. dia charcoal fiberglass	Charcoal-black	0.58

The infrared spectra are automatically averaged and integrated with respect to the back body spectrum at selectable temperature range. Emittance values are evaluated from the integrated values of the spectral reflectance. Detailed description and the operating principles of the SOC 400T is documented by Surface Optics Corporation (2002) and Jaworske and Skowronski (2000).

The SOC 400T is the current state-of-the-art instrument that may be offered as a substitute for the well known Gier Dunkle DB-100 infrared reflectometer. This is because the SOC 400T has the capability to measure reflectance over a large spectral range and subsequently evaluates emittance over a large temperature range. The Gier Dunkle DB-100, on the other hand, measures total reflectance in the vicinity of 9.7 μm while emittance can only be evaluated at room temperature. Another remarkable difference between the two instruments is that the DB-100 measures hemispherical-normal reflectance whereas the SOC 400T measures normal-hemispherical reflectance.

Measurements

As stated at the onset, the SOC 400T is designed to measure infrared reflectance of samples that are opaque to infrared radiation. However, by following a general theory and measurement procedure documented by Christie and Hunter (1984), the reflectometer can be adapted to measure both infrared reflectance and transmittance of diathermanous samples. Emittance is easily estimated from the reflectance and the transmittance measurements.

The SOC 400T was calibrated by first leaving the measurement port uncovered while the room was scanned and the zero spectrum recorded. Care was taken not to obstruct the field of view of the measurement port. A specular gold disk was then placed over the measurement port and the reference spectrum recorded. The gold disk has a constant reflectance value of 0.98 in the wavelength range of $2.0 < \lambda < 25.0$ μm. To confirm this reflectance value, a reflectance measurement was obtained after calibration while the gold disk was still in place. This confirmation was necessary since the gold disk also served as a backing surface. As such, its reflectance value needed to be known accurately. The reflectance of a second backing surface (black surface) was also measured and found to be 0.07.

Having obtained the calibration spectra and the reflectance values of the two backing surfaces, two sets of spectral reflectance measurements were taken for each sample listed in Tables 1, 2 and 3. The first set of measurements was obtained by placing the sample over the measurement port with the gold surface backing it. The second set of measurements was obtained by replacing the gold surface with the black surface. In both cases, the total emittance of the opaque surface formed by the sample and the backing surface were computed from the spectral reflectance measurements at temperatures ranging from 290 to 300 K.

ESTIMATION OF EMITTANCE AND LONGWAVE TRANSMITTANCE

Consider longwave radiation incident on the surface of a given sample. Assuming the sample is grey, the total reflectance, ρ, the total transmittance, τ and the total emittance, ε, are related by principle of energy conservation and Kirchoff's law,

$$\rho = 1 - \tau - \varepsilon \qquad (1)$$

For an opaque sample, $\tau = 0$ and

$$\rho = 1 - \varepsilon \qquad (2)$$

The SOC 400T measures the spectral reflectance of an opaque surface, integrates the spectral data with respect to black body spectrum at a given temperature and computes ε. The value of ρ can subsequently be calculated from Equation 2.

To estimate ε and τ of a diathermanous sample, we resort to the procedure outlined by Christie and Hunter (1984). Christie and Hunter used theoretical analysis to derive reflectance equations by considering radiation incident on a thin diathermanous film backed by two different surfaces. The system (i.e., the diathermanous film together with the backing surface) reflectance in each case is dependent on the film and the backing surface reflectance values as well as the film transmittance. Given the reflectance values of the backing surfaces, the film reflectance, ρ and the film transmittance, τ were obtained as

$$\rho = \frac{(\rho_{B1}/\rho_{B2})\rho_{M2} - \rho_{M1}}{(\rho_{B1}/\rho_{B2}) + \rho_{B1}(\rho_{M2} - \rho_{M1}) - 1} \qquad (3)$$

and

$$\tau = \sqrt{\frac{(\rho_{M1} - \rho)(1 - \rho\rho_{B1})}{\rho_{B1}}} \qquad (4)$$

where ρ_{M1} and ρ_{M2} are the system reflectance values with backing surfaces 1 and 2 in place while ρ_{B1} and ρ_{B2} are the reflectance values of backing

surfaces 1 and 2. Having obtained ρ and τ, ε can be calculation from Equation (5)

$$\varepsilon = 1 - \tau - \rho \quad (5)$$

Equations 4 and 5 give the values of ε and τ for each shading material summarised in Tables 1, 2 and 3. The following subsections describe the functional dependence of ε and τ on A_o for each class of shading material.

Drapery Fabrics

To establish a relationship between ε and A_o, measured values of ε were plotted against $1 - A_o$ as shown in Figure 1(a). Note that values of A_o were obtained from solar optical measurements (Kotey et al. 2009a). Equation 6 is the result of a regression fit (goodness of fit, R-squared = 0.94) obtained from the measured data.

$$\varepsilon = 0.87(1 - A_o) \quad (6)$$

The straight line shown in Figure 1(a) represents Equation 6. Clearly, there is a strong correlation between ε and $1 - A_o$. The regression fit was set to pass through the origin since in the limit where $A_o \to 1$ (i.e., the fabric disappears) $\varepsilon \to 0$ and Equation 6 correctly satisfies this limiting case.

A similar relationship was established between τ and A_o by plotting values of $1 - \tau$ against $1 - A_o$. See Figure 1(b). Equation 7 is the result of a regression fit (goodness of fit, R-squared = 0.95) obtained from the plot.

$$1 - \tau = 0.95(1 - A_o) \quad (7)$$

Again, there exists a strong correlation between τ and A_o as seen in Figure 1(b). The straight line shown in Figure 1(b) representing Equation 7 passes through the origin since in the limit where $A_o \to 1$, $\tau \to 1$. Substituting $1 - A_o$ from Equation 7 into Equation 6 gives the desired relationship between ε and τ, i.e.,

$$\varepsilon = 0.92(1 - \tau) \quad (8)$$

To confirm this relationship, measured values of ε were plotted against $1 - \tau$ as shown in Figure 1(c). A regression fit (goodness of fit, R-squared = 0.99) given by Equation 8 was indeed realised. Such a strong correlation further validates the relationships established between longwave properties and openness.

Roller Blinds

The measured values of ε were plotted against $1 - A_o$. See Figure 2(a). Values of A_o were again obtained from solar optical measurements reported by Kotey et al. (2009b). The best possible regression fit that passes through the origin is given

$$\varepsilon = 0.91(1 - A_o) \quad (9)$$

Equation 9 establishes the relationship between ε and A_o. To establish a similar relationship between τ and A_o, values of $1 - \tau$ were plotted against $1 - A_o$ as shown in Figure 2(b). Again, a linear regression fit was obtained as given by Equation 10.

$$1 - \tau = 0.95(1 - A_o) \quad (10)$$

Again, substituting $1 - A_o$ from Equation 10 into Equation 9 gives the desired relationship between ε and τ, i.e.,

$$\varepsilon = 0.96(1 - \tau) \quad (11)$$

A plot of the values of ε against $1-\tau$ fall on the straight line represented by Equation 11 and confirms the relationship between ε and τ. See Figure 2(c).

Insect Screens

Once again, values of ε were plotted against $1 - A_o$ in order to establish a relationship between ε and A_o. See Figure 3(a). Values of A_o were again obtained from solar optical measurements reported by Kotey et al. (2009c). For a given range of A_o, it is seen from Figure 3(a) that dark screens showed consistently higher values of ε compared to shiny screens. It was therefore logical to distinguish between dark and shiny screens in the subsequent analysis.

Two different regression fits deduced from the plots in Figure 3(a) are Equation 12 for dark screens and Equation 13 for shiny screens, i.e.,

$$\varepsilon = 0.93(1 - A_o) \quad (12)$$

$$\varepsilon = 0.32(1 - A_o) \quad (13)$$

Although the regression fits were not quite great, they represented the measured data to a reasonable accuracy.

Turning consideration to the relationship between τ and A_o, measured values of $1 - \tau$ were plotted against $1 - A_o$ as shown in Figure 3(b). Again, there was a discernible difference between the data set obtained for dark and shiny screens. The correlation between $1 - \tau$ and $1 - A_o$ for dark and shiny screens as established by regression fits are given by Equations 14 and 15, respectively.

$$1 - \tau = 0.98(1 - A_o) \quad (14)$$

$$1 - \tau = 0.81(1 - A_o) \quad (15)$$

The straight lines representing these correlations are also shown in Figure 3(b).

Finally, it can readily be shown that for dark and shiny screens, ε is directly related to τ via Equations 16 and 17, respectively, i.e.,

$$\varepsilon = 0.95(1 - \tau) \quad (16)$$

$$\varepsilon = 0.40(1 - \tau) \quad (17)$$

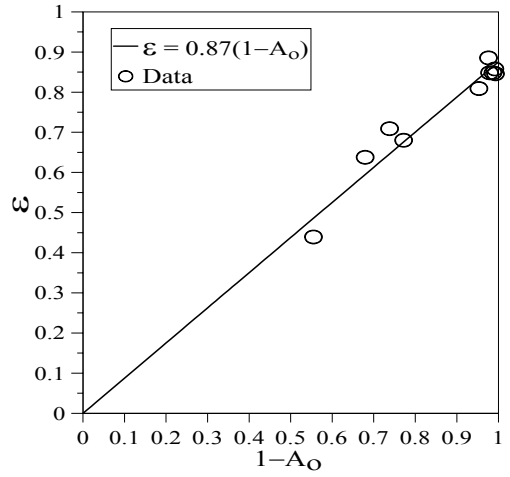

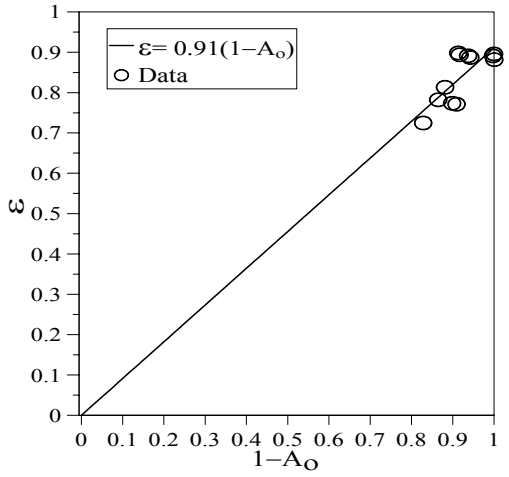

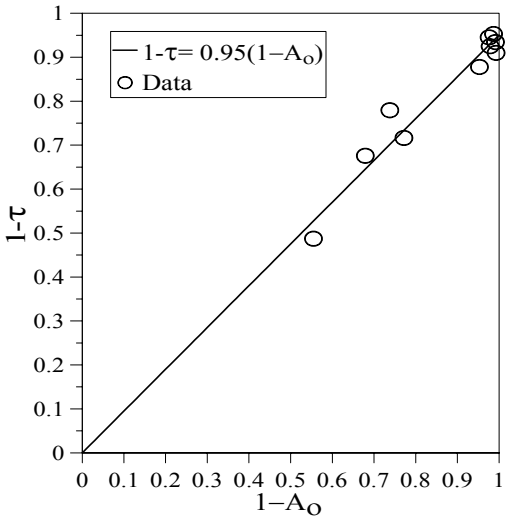

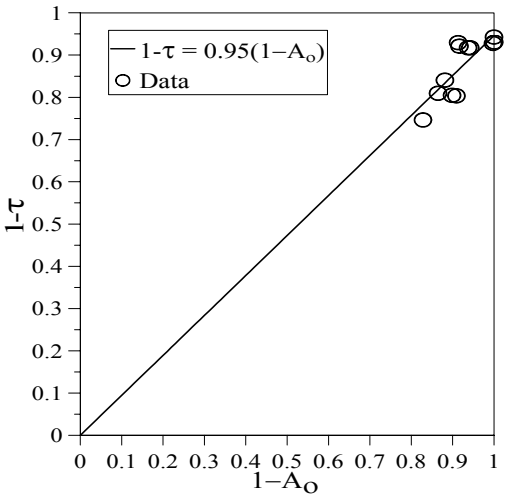

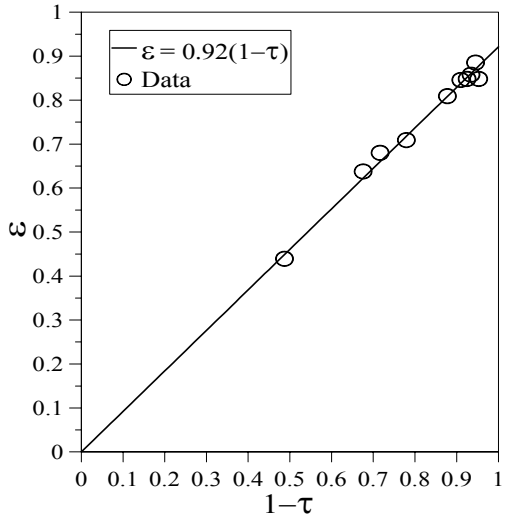

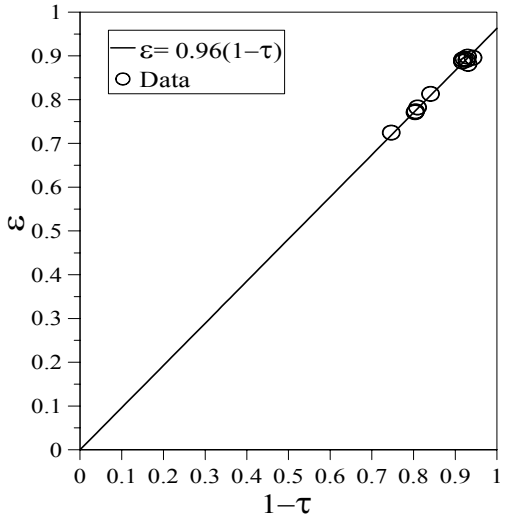

Figure 1. Longwave Radiative Properties of Drapery Fabrics
(a) ε versus (1-A_O) (b) (1-τ) versus (1-A_O) (c) ε versus (1-τ)

Figure 2. Longwave Radiative Properties of Roller Blinds
(a) ε versus (1-A_O) (b) (1-τ) versus (1-A_O) (c) ε versus (1-τ)

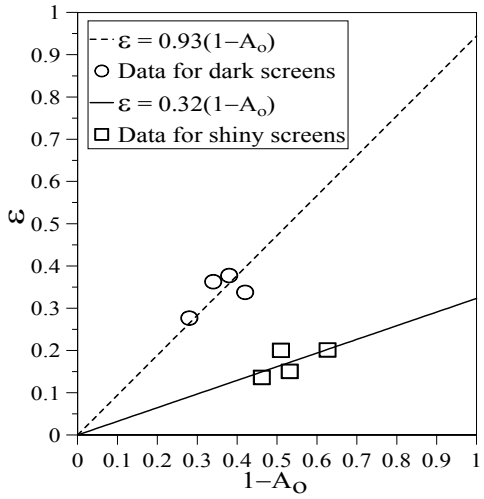

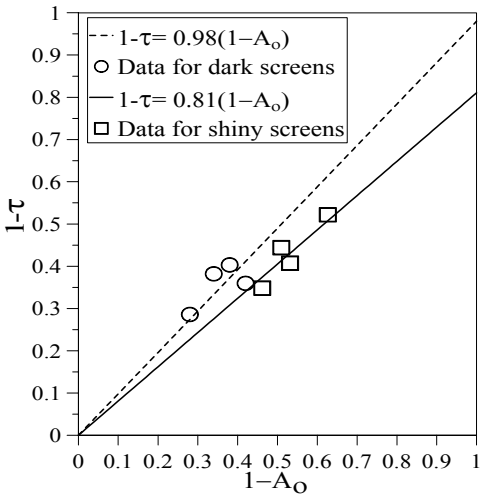

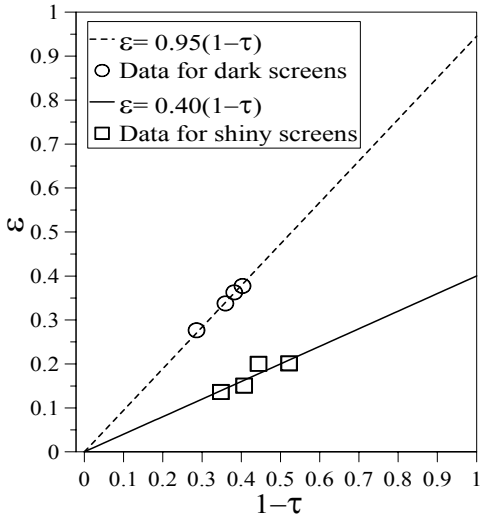

Figure 3. Longwave Radiative Properties of Insect Screens (a) ε versus (1-A_O) (b) (1-τ) versus (1-A_O) (c) ε versus (1-τ)

To reaffirm this relationship, values of ε were plotted against $1-\tau$ as shown in Figure 3(c). Again, regression fits established by Equations 16 and 17 show a strong correlation between ε and τ.

DISCUSSION

The coefficients in Equations 6, 9, 12 and 13 may be considered to be the total hemispherical emittance of the structure making up the fabric, the roller blind, the dark screens and the shiny screens, respectively. This is because when $A_o = 0$, the emittance of the shading material is simply equal to the emittance of the structure. The measurements show that irrespective of the colour of the fabric, the emittance of the fabric structure may be considered to be constant. The same observation is apparent for the emittance of the roller blind structure. Insect screens, on the other hand, show two distinct structural emittance values depending on the surface finish. The structural emittance of a dark screen is much higher than that of a shiny screen.

Table 4 summarises the estimated total hemispherical emittance, transmittance and reflectance of the structure of each shading material. Also shown in Table 4 are the total normal emittance values of typical opaque surfaces at specified temperatures (Modest 1993, Siegel and Howell 1993, Incropera and DeWitt 2001). Note that hemispherical emittance can be estimated from the normal emittance values. Materials with high emittance tend to behave like dielectrics and therefore have a hemispherical emittance that is 3 to 5% greater than the normal emittance. On the other hand, metals generally have a hemispherical emittance that is 3 to 10% greater than the normal emittance (Modest 1993, Holland 2004). From the literature survey, it is obvious that a typical fabric made from dyed cloth has a high emittance which is independent of the colour of the dye (paint). Furthermore, roller blinds which are generally made from plastics and paint also have high emittance values independent of the colour of the paint. The same observation can be made for the high emittance values of dark screens. However, the emittance of shiny screens is attributed to the emittance of the stainless steel. Since metals generally have low emittance values, the shiny stainless steel screens will also exhibit low emittance.

Consideration will now turn to the behaviour of longwave transmittance of the shading materials when $A_o = 0$. From Equations 7, 10, 14 and 15, it is evident that the τ value of a shading material does not necessarily drop to zero under such circumstances. Substituting $A_o = 0$ into the aforementioned equations give the τ values of the

Table 4. Summary of longwave properties

Experimental Results				Results from Literature Survey		
Shading Material	**Estimated hemispherical emittance of structure at 300 K**	**Estimated hemispherical transmittance of structure**	**Estimated hemispherical reflectance of structure**	**Opaque surfaces**	**Surface temp (K)**	**Typical total normal emittance**
Fabrics	0.87	0.05	0.08	Paint (all colours)	300	0.92-0.98
Roller blinds	0.91	0.05	0.04	Cloth	293	0.77-0.78
Dark (painted stainless steel) screens	0.93	0.02	0.05	Plastics	291	0.84-0.95
Shiny (unpainted stainless steel) screens	0.32	0.19	0.49	Stainless steel (various types)	368	0.27-0.42

structure. The results are summarised in Table 4. The finite value of τ when $A_O = 0$ may be attributed to multiple reflections between structural members of each shading material (i.e., yarn, wire, sheet) and subsequent transmission through the interstices of the structure. To further substantiate this argument, the ρ value of the structure was estimated from Equation 1 given the values of τ and ε. The results are also included in Table 4. It is clearly seen from Table 4 that fabrics, roller materials and dark screens with low values of ρ have low values of τ. On the other hand, shiny screens with relatively high value of ρ have a high value of τ.

CONCLUSIONS

A method of estimating the longwave radiative properties of flat shading materials like drapery fabrics, insect screens and roller blinds is reported. The method involved the use of a portable infrared reflectometer originally designed to measure the emittance of opaque surfaces. The shading materials considered consists of a structure (i.e., yarn, wire, sheet) that is opaque with respect to longwave (infrared) radiation and each material is likely to have some openness. Two backing surfaces were therefore used in the measurements in order to estimate both emittance and longwave transmittance of each shading material. It was found that the emittance and longwave transmittance are simple functions of openness as well as the emittance and longwave transmittance of the structure. The results are particularly useful since openness can be determined from solar transmittance measurements while emittance and longwave transmittance of the structure was found to be constant for each category of shading material. The results offer significant value in modeling these shading materials in the context of building energy simulation.

ACKNOWLEDGEMENTS

We would like to thank NSERC and ASHRAE for their financial support. We would also like to thank Shade-O-Matic for supplying us with roller blind samples.

NOMENCLATURE

Symbols

A_o	openness

Greek Letters

α	absorptance (dimensionless)
ε	emittance (dimensionless)
λ	wavelength (m)
ρ	reflectance (dimensionless)
τ	transmittance (dimensionless)

Subscripts

bb	beam-beam solar property

Abbreviations

ASHRAE	American Society of Heating, Refrigerating and Air Conditioning Engineers
ASTM	American Society for Testing and Materials
FTIR	Fourier Transform Infrared Spectroscopy
HVAC	Heating, Ventilating and Air Conditioning
NSERC	Natural Sciences and Engineering Research Council of Canada

REFERENCES

ASTM E408-71. 1971. *Standard Test Method for Total Normal Emittance of Surfaces Using Inspection-Meter Techniques*. Philadelphia: American Society for Testing and Materials.

Christie, E.A. and A.J. Hunter. 1984. Total infrared radiation property measurements of diathermanous films with a reflectometer. Solar Energy, 33(6): 613-618.

Hollands, K.G.T. 2004. *Thermal Radiation Fundamentals*. Begell House, Inc, New York.

Incropera, F.P. and D.P. DeWitt. 2001. *Fundamentals of Heat and Mass Transfer*. 5th Eddition. John Wiley and Sons, Inc.

Jaworske, D.A. and T.J. Skowronski. 2000. Portable infrared reflectometer for evaluating emittance. *Proceedings of the Space Technology and Applications International Forum, Albuquerque, New Mexico, pp. 791-796*.

Keyes, M.W. 1967. Analysis and rating of drapery materials used for indoor shading. ASHRAE Transactions, 73, (1): 8.4.1.

Kotey, N.A., Collins, M.R., Wright, J.L., and T. Jiang. 2008. A simplified method for calculating the effective solar optical properties of a venetian blind layer for building energy simulation. Accepted for Publication in ASME Journal of Solar Energy Engineering.

Kotey, N.A., Wright, J.L. and M.R. Collins. 2009a. Determining off-normal solar optical properties of drapery fabrics. ASHRAE Transactions, 117(1)

Kotey, N.A., Wright, J.L. and M.R. Collins. 2009b. Determining off-normal solar optical properties of roller blinds. ASHRAE Transactions, 117(1).

Kotey, N.A., Wright, J.L. and M.R. Collins. 2009c. Determining off-normal solar optical properties of insect screens. ASHRAE Transactions, 117(1).

Kotey, N.A., Wright, J.L. and M.R. Collins. 2009d. A detailed model to determine the effective solar optical properties of draperies. ASHRAE Transactions, 117(1).

Modest, M.F. 1993. *Radiative Heat Transfer*. McGraw-Hill, Inc.

Parmelee, G. V. and W.W. Aubele., The shading of sunlit glass: an analysis of the effect of uniformly spaced flat opaque slats. ASHVE Transactions, 58: pp. 377-398.

Pfrommer, P., Lomas, K.J., and Chr. Kupke.1996. Solar radiation transport through slat-type blinds: A new model and its application for thermal simulation of buildings. Solar Energy. 57(2): 77-91.

Rheault, S.; E. Bilgen, 1989, Heat transfer analysis in an automated venetian blind system, Journal of Solar Energy, Vol. 111 (Feb.), pp. 89-95.

Rosenfeld, J.L.J., Platzer, W.J., Van Dijk, H., and Maccari, A., (2000) "Modelling the Optical and Thermal Properties of Complex Glazing: Overview of Recent Developments", Solar Energy, Vol. 69 Supplement, No. 1-6, pp.1-13.

Siegel, R. and J.R. Howell. 1993. *Thermal Radiation Heat Transfer*. 3rd Edition. Taylor and Francis Inc.

Surface Optics Corporation. 2002. *SOC 400T User Guide*. San Deigo, CA.

Wright, J.L., and Kotey, N.A., 2006. Solar Absorption by Each Element in a Glazing/Shading Layer Array. ASHRAE Transactions, 112(2): 3-12.

Yahoda, D.S., Wright, J.L., "Methods for Calculating the Effective Longwave Radiative Properties of a Venetian Blind Layer," ASHRAE Transactions, Vol. 110, Pt. 1., pp. 463-473 (2004).

Yahoda, D.S. and J.L. Wright. 2005. Methods for calculating the effective solar-optical properties of a venetian blind layer. ASHRAE Transactions, 111(1): 572-586.